

“Robotrac” Mobile 6R Closed Chain

P.J. Zsombor-Murray

McGill University, Department of Mechanical Engineering

Anton Gferrer

TU-Graz, Institut für Geometrie

Abstract: Two noncolinear, parallel axis revolute joints each form an axle and bearing for one of the two driven wheels which, together with two prismaticly actuated legs, support and propel a vehicle designed as a platform for off-road timber harvesting, excavation and construction machinery. The wheel-ground contacts are modeled as universal or U-joints. Such a closed chain model reveals a mobile 6R mechanism wherein the centres of the two axle R-joints, indeed the entire line connecting these centres, describe single degree of freedom motion and move on an eighth order spherical curve with three mutually orthogonal planes of symmetry.

Resumé: Deux articulations rotatives d'axe à manivelle supportent les deux roues actionnées d'un véhicule hors-piste amélioré par l'ajout de deux jambes articulées et actionnées aux cylindres hydraulique. Ces véhicules s'emploient dans le boisé, l'excavation et le bâtiment. On modélise les contacts entre roue et terre par des articulations Cardan. Le système de roues-axe-terre comprend une boucle mobile à 6R fermée; un mécanisme de surcontraint et d'inédit. Imaginez les points d'intersection entre chaque axe de roue et le rayon vers le point de contact à terre. On a trouvé que les points sur la ligne, au

travers de ces points, se déplacent sur courbes sphériques, de l'ordre de huit, possédant de trois plans de symétrie orthogonale.

Introduction: Hiller and Schmitz [5], Kecskeméthy [7], Hiller *et al* [6] and Six and Kecskeméthy [8] treated the design, construction, kinematics, dynamics and control of a wheeled-and-legged striding vehicle called *Robotrac*; a sort of mechanized rickshaw. However only the latter [8] alludes to an over-constrained, single loop, six-revolute joint single closed chain mechanism. This mechanism presented itself as the authors analyzed self-steering properties of the wheel pair when the vehicle negotiates uneven terrain. Wheel bearing axes are not colinear but, though parallel, offset so the two axles and an intersecting perpendicular describe a simple, planar crank. Wheels accommodate irregular terrain by powered rotation of the crank so as to change the distance ratio of the axles with respect to the vehicle platform plane. Unless the plane of the crank is vertical, so as to maximize the ratio, one wheel contact point is generally ahead of the other. Furthermore a ground surface tangent plane is usually not parallel to the wheel axle. An important result of the analysis [8] was to show that the dihedral angle between the wheel and tangent

planes has little or no effect on turning sense or tendency. Moreover self steering occurs in a direction such that the trailing wheel, with respect to direction of vehicle advance, is on the smaller turning radius while the leading one follows an arc of greater radius.

The Overconstrained Mechanism: It is not the purpose here to pursue the non-holonomic rolling characteristics of this two-wheel set which was described by Six & Kecskeméthy [8]. Rather, consider the type of conceptual mechanism that is often used to model such behaviour. Referring to the upper drawing in Fig. 1 one sees the two wheels with their ground contact points modeled as universal or Cardan joints, U-joints, where both axes are in the wheel plane, one through the revolute, R-joint wheel bearing centre, the other perpendicular to the first. Notice the crank axle which is placed in a reference position with the R-joint axes respectively perpendicular to the first U-joint axes mentioned above. Now the lower drawing in Fig. 1 again shows all components in reference or “home” position. The wheel is represented by a *spoke link line* which connects wheel bearing R-joint and ground contact U-joint centres. The virtual U-joints are expressed explicitly here. Note the placement of the Cartesian reference frame and the three design parameters a , b and c . The mobility of this mechanism will be analyzed as the motion of the R-joint centre whose home position is on the z -axis shown.

Analysis: Examine Fig. 1 again. This system should not be mobile. It is a spatial four-bar configuration consisting of the ground, two wheel “spokes” and the crank axle. There are two R-joints which each remove five degrees of freedom(dof) from the system while the U-joints each constrains four dof. This gives a total of

$$\sum C_j = (2 \times 5) + (2 \times 4) = 18$$

system constraints. Given $S = 6$, the number of dof in three dimensional space, and the number of movable links

$$(N - 1) = (4 - 1) = 3$$

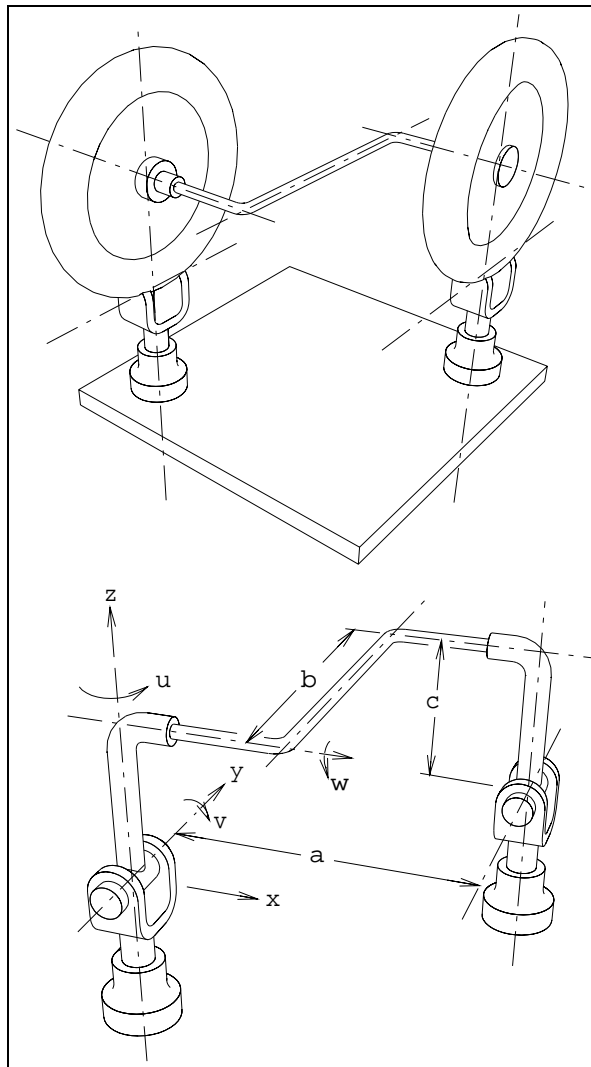


Figure 1: Wheel & Crank Model

the Chebychev-Grubler-Kutzbach relation produces a theoretical mobility of

$$M = S(n - 1) - \sum C_j = 6(4 - 1) - 18 = 0$$

Mobility Hypothesis: Let us, for the moment, remove the crank axle and observe the

spherical motion of the two axle bearing R-joint centres. They must move so that their axes remain parallel. Parameterize the motion on an independent angle variable u which has a positive vector along the z -axis. Thus the left hand R-joint axis branch in the positive x -direction will turn, with positive u towards the y -axis. For any value of angle u the R-joint axis will turn by a dependent angle v about the U-joint axis initially aligned on the y -axis. A positive rotation through angle v will cause the positive branch of the R-joint axis to dip as the R-joint centre moves along a meridial circle, polar on the z -axis and whose position is measured by longitude u . The dependency of v upon u is necessary to maintain compatibility with the crank since for any $u \neq 0$ the meridial planes are no longer separated by distance b . Because of this, the crank rotation angle w must be considered. This is defined, with respect to the reference or “home” position as a positive rotation vector in the x -direction so as to raise the parallel R-joint axis passing through the right hand R-joint.

Assembly, Symmetry, Compatibility, Mobility: Clearly, one may assemble some arbitrary combination of design parameters. For purposes of detailed illustration length dimensions $a = 24$, $b = 6$, $c = 16$ were used. These are shown in Fig. 1. Although not immediately obvious, it will be seen that spherical displacement characteristics depend solely on the dimensionless ratio b/a . On the other hand it *is* immediately obvious that when $u = \tan^{-1}(b/a)$ the two meridial planes coincide. Both R-joint axes fall into this vertical plane and $v = u$ so that the distance between the two spoke lines is maintained at a and the R-joint axial separation is maintained at b . This establishes another assembly mode; not quite mobility but at least one can see how the crank axle must assume a vertical pose when the parallel meridial circle planes

coincide and thus have no distance separating them. This situation is illustrated in the lowermost auxiliary view in Fig. 3. The ability to exhibit auxiliary elevations at arbitrary angles u which maintain crank compatibility is the key to establishing mobility and analyzing the nature of displacement.

Angular Relations: Four auxiliary elevation views are shown in Fig. 2.

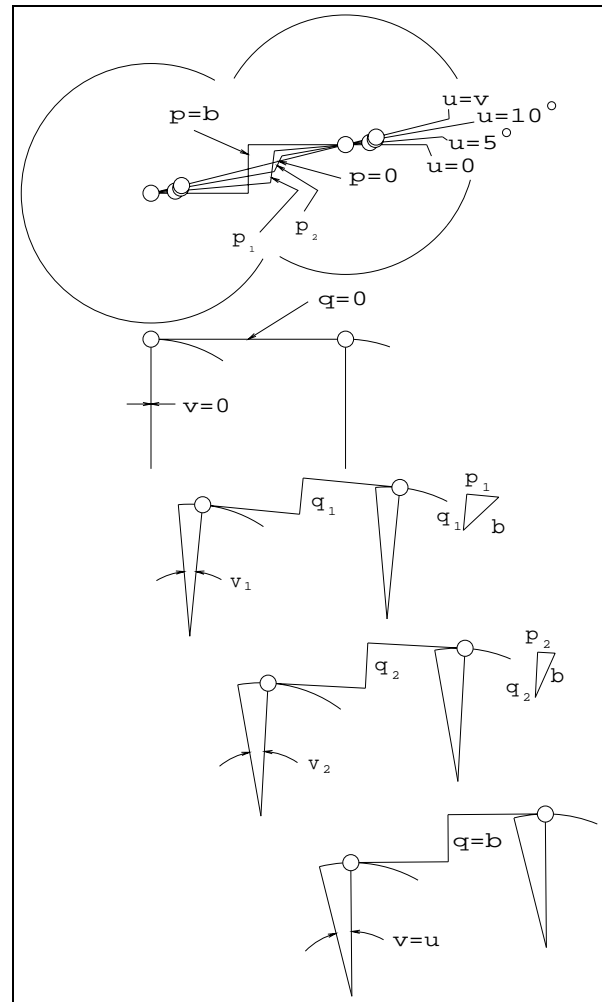


Figure 2: Movement of the Crank Axle

The first shows the reference position where $u = v = 0$ and the fourth shows a maximum value of v such that $v = u = \tan^{-1}(b/a)$. But in between we see situations where the

meridial planar separation, a horizontal distance measured in the top view as a projection on the plane $z = 0$, is $b > p > 0$. In the auxiliary views one sees the distance q which is the component of R-joint axis separation projected onto the auxiliary vertical meridial plane with homogeneous coordinates

$$m_O\{0 : \cos u : -\sin u : 0\}$$

Obviously $p^2 + q^2 = b^2$ and similarly the spoke line separations measured in all five auxiliary view remains fixed at a . This does not quite constitute formal mathematical rigor concerning proof of mobility but it is felt that the argument is conclusive, nonetheless.

Simple Trigonometry: Deriving the angular relations for $\cos v$ and $\cos w$ is quite straight forward. We start by removing the example from Fig. 2, where $u = 5^\circ$, and enlarging and labeling it as shown in Fig. 3.

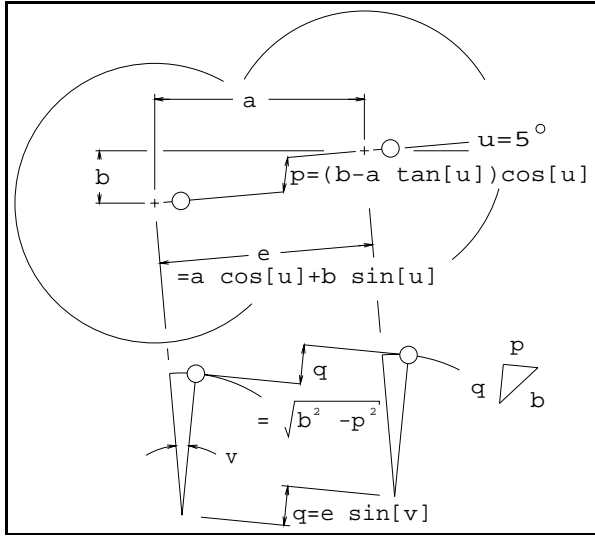


Figure 3: Distance & Angle Relations

The expressions for the distance p

$$p = (b - a \tan u) \cos u$$

for the distance e which separates U-joints projected on to meridial plane

$$e = a \cos u + b \sin u$$

and two for the distance q

$$q = e \sin v = \sqrt{b^2 - p^2}$$

are easy to determine by examining Fig. 3 and are all that is needed. To get w is easier. One notes

$$\begin{aligned} \cos w &= \frac{p}{b} = \frac{(b - a \tan u) \cos u}{b} \\ &= \frac{b \cos u - a \sin u}{b} \end{aligned} \quad (1)$$

Then from the two relations for q we may write

$$\begin{aligned} &(a \cos u + b \sin u)^2 \sin^2 v \\ &= b^2 - (b \cos u - a \sin u)^2 \end{aligned}$$

Replacing $\sin^2 u$ with $1 - \cos^2 u$, expanding and simplifying produces

$$\cos v = \frac{a}{a \cos u + b \sin u} \quad (2)$$

Both Eq. 2 and Eq. 1 may be nondimensionalized to functions of the ratio $r = b/a$. Notice the spoke length c appears nowhere.

$$\sec v = \cos u + r \sin u \quad (3)$$

$$\cos w = \cos u - \frac{\sin u}{r} \quad (4)$$

If relationships between v and w are desired one may substitute

$$\sin^2 u = 1 - \cos^2 u$$

in Eqs. 3 and 4

$$\cos u + r \sqrt{1 - \cos^2 u} - \sec v = 0$$

$$\cos u - \frac{\sqrt{1 - \cos^2 u}}{r} - \cos w = 0$$

and eliminate $\cos u$ to obtain Eq. 5, a fourth order polynomial in $\cos w$ which can be solved explicitly if required.

$$\begin{aligned} v_0 \cos^4 w + v_1 \cos^3 w + v_2 \cos^2 w \\ + v_3 \cos w + v_4 = 0 \end{aligned} \quad (5)$$

where

$$\begin{aligned} v_0 &= r^4(r^2 + 1)^2 \\ v_1 &= -4r^4(r^2 + 1) \sec v = r_1 \sec v \\ v_2 &= -2r^2 \{[(r^4 - 1) - 2r^2] \sec^2 v \\ &\quad - r^2[r^2(r^2 + 1) - 1] - 1\} \\ &= r_2 \sec^2 v + r_0 \\ v_3 &= 4r^2(r^2 - 1)[\sec^3 v - (r^2 + 1) \sec v] \\ &= r_3 \sec^3 v + r'_1 \sec v \\ v_4 &= (r^2 - 1)^2 \sec^4 v \\ &\quad - \{2[r^2(r^2 - 1) - 1] + 1\} \sec^2 v \\ &\quad + [(r^4 - 1)^2 - r^5(r^2 - 1)] \\ &= r_4 \sec^4 v + r'_2 \sec^2 v + r'_0 \end{aligned}$$

Alternately, Eq. 5 can be rearranged in order to be solved for v .

$$\begin{aligned} r_4 \sec^4 v + r_3 \cos w \sec^3 v \\ + (r_2 \cos^2 w + r'_2) \sec^2 v \\ + (r_1 \cos^3 w + r'_1 \cos w) \sec v \\ + (v_0 \cos^2 w + r_0 + r'_0) = 0 \end{aligned} \quad (6)$$

Notice that the reciprocal $\sec v$ can be replaced with $\cos v$ by multiplying Eqs. 5 and 6 by $\cos^4 v$.

Implicit Form and Results: Although the distance c does not appear in the solution, Eq. 3, one must assume *some* radius for the spoke sphere centred on an R-joint in order to obtain the implicit equation of the spoke cone, *i.e.*, the surface swept out by a spoke line. First we note the polar *-vs-* Cartesian relationships.

$$\begin{aligned} x = c \cos u \sin v &\Rightarrow \cos u = \frac{x}{c \sin v} \\ y = c \sin u \sin v &\Rightarrow \sin u = \frac{y}{c \sin v} \\ z = c \cos v &\Rightarrow \cos v = \frac{z}{c} \end{aligned}$$

These can be substituted into Eq. 3 to produce

$$\frac{c}{z} = \frac{x}{c \sin v} + \frac{by}{ac \sin v}$$

This expands to

$$(x + by/a)^2 z^2 + c^2(z^2 - c^2)$$

which together with the sphere

$$x^2 + y^2 + z^2 - c^2 = 0 \quad (7)$$

gives the fourth order surface, a cone with its apex on the origin.

$$[(x + \frac{b}{a}y)z]^2 - (x^2 + y^2 + z^2)(y^2 + z^2) = 0 \quad (8)$$

The eighth order curve of the R-joint trajectory is obtained with all simultaneous solutions of Eq. 7 and Eq. 8. Finally we see in Fig. 4 a projection of such curves on $z = 0$ for $b/a = 6/24, 12/24, 24/24, 48/24$.

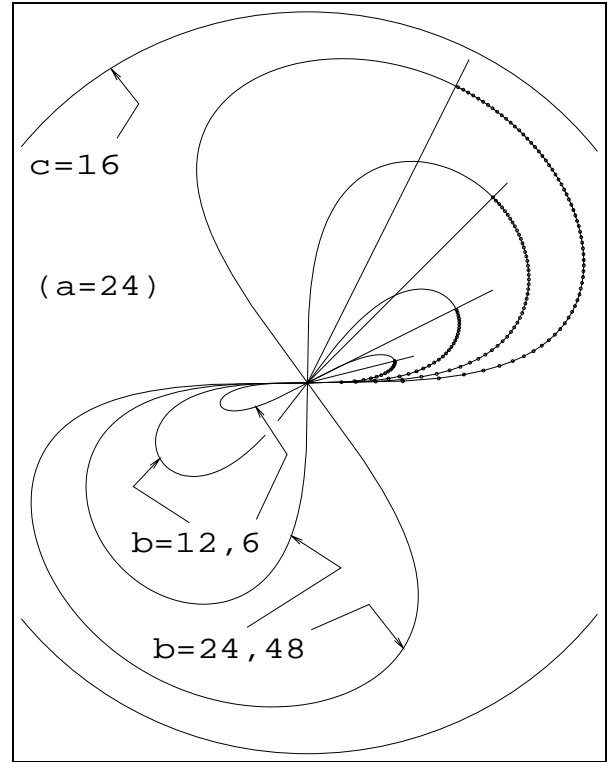


Figure 4: Spherical Self-Motion Curves

These were produced not from the implicit relations but from Eq. 2, varying u by one degree increments and computing v , then plotting x and y from the first two polar to Cartesian relationships above.

Planes of Symmetry: The planes of symmetry of the figure eight-like intersections of the cone and sphere are easy to see. These are:-

- The equatorial plane $z = 0$ which separates the cone into halves on the apex,
- The meridial planes $m\{0 : -b : a : 0\}$ and
- The meridial planes perpendicular to m , $n\{0 : a : b : 0\}$.

Conclusion: The self motion of this mechanism, apart from revealing an apparently novel 6R closed chain, should contribute something to the understanding of *Robotrac* steering behaviour, *i.e.*, what sort of tracking radius may be expected, given a steering input angle w to a mechanism with a design specified by a, b, c .

Of possible interest to the community of geometricians, it is satisfying to note that, notwithstanding the eighth order R-joint trajectory curve, really two diametrically opposite fourth order curves on the sphere surface, and the fourth order cone swept by the spoke line, given the mechanism's design parameters a, b, c and a specific value of angle u , the angles v and w can be obtained constructively. So the computation can be reduced to quadratic equation solving. This was illustrated in Fig. 3. A mechanism with $a = 24$, $b = 6$ and $c = 16$ was shown with an arbitrary selection of $u = 5^\circ$. The distance p can be measured immediately in the top view as the distance between the meridial circle planes at longitude uE , assuming the plan is viewed from the north pole. Then q

can be found with a right angle triangular construction where p is one side and b is the hypotenuse. Finally the angle v is available in the auxiliary elevation of the meridial circle planes. It is only necessary to construct the common tangent between one of the meridial circles and another of radius $c - q$ concentric with the second meridial circle. The tangent dips v from the horizontal.

It is noted with satisfaction that Dietmaier's extensive lexicon [3] of mobile over-constrained single loop spatial 6R mechanisms does not include this one. Not too surprising because, unlike the unique Bennett four jointed loop [1] and the relatively rare five jointed "Goldberg Variations" [4] (apologies to the late Glen Gould), six jointed loop species are common and continue to defy complete classification. Nevertheless the Denavit-Hartenberg parameters [2] of this one are cited below, for the record. We go around the loop starting with the vertical axis R-joint that defines the meridial angle u of the grounded U-joint on the left.

$$\begin{array}{lll}
 \alpha_1 = \frac{\pi}{2} & a_1 = 0 & s_1 = 0 \\
 \alpha_2 = \frac{\pi}{2} & a_2 = c & s_2 = 0 \\
 \alpha_3 = 0 & a_3 = b & s_3 = a \\
 \alpha_4 = \frac{\pi}{2} & a_4 = c & s_4 = 0 \\
 \alpha_5 = \frac{\pi}{2} & a_5 = 0 & s_5 = 0 \\
 \alpha_6 = 0 & a_6 = \sqrt{a^2 + b^2} & s_6 = 0
 \end{array}$$

Acknowledgements: This research is supported by grants provided by NSERC 139964, Natural Sciences and Engineering Research Council (Canada) and FCAR ER73234, Fonds pour la Formations des Chercheurs et l'Aide à la Recherche (Québec).

References

- [1] Bennet, G.T. (1903): “A New Mechanism”, *Engineering*, 1903-09, pp.777-778.
- [2] Denavit, J. & Hartenberg, R.S. (1955): “A Kinematic Notation for Lower-Pair Mechanisms Based on Matrices”, *ASME J. Appl. Mech.*, v.22, pp.215-221.
- [3] Dietmaier, P. (1995): “Einfach übergeschlossene Mechanismen mit Drehgelenken”, *Habilitationschrift*, TU-Graz, Institut f. Mechanik.
- [4] Goldberg, M. (1943): “New Five-Bar and Six-Bar Linkages in Three Dimensions”, *Trans. ASME*, 1943-08, pp.649-661.
- [5] Hiller, M. & Schmitz, T. (1990): “Kinematics & Dynamics of the Combined Legged & Wheeled Vehicle ‘Robotrac’ ”, *Proc. CSME Forum '90*, v.3, Toronto, 90-06-(03→09), pp.387-392.
- [6] Hiller, M., Schweitzer, G. & Wornle, C. (1990): “Kinematical Control of the Wheeled & Legged Vehicle ‘Robotrac’ ”, *Proc. RoManSy 8th CISM-IFTOMM Symposium*, Morecki, A., Bianci, G. & Jaworek (eds.), Hermes, ISBN 83-900501-2-9, Cracow, 90-07-(02→05), pp.310-319.
- [7] Kecskeméthy, A. (1994): “A Spatial Leg Mechanism with Anthropomorphic Properties for Ambulatory Robots”, *Advances in Robot Kinematics & Computational Geometry*, Lenarčič, J. & Ravani, B. (eds.), Kluwer, ISBN 0-7923-2983-X, pp.161-170.
- [8] Six, K. & Kecskeméthy, A. (1999): “Steering Properties of a Combined Wheeled & Legged Striding Excavator”, *Proc. 10th IFTOMM World Congress*, v.1, ISBN 951-42-5287-X, Oulu, 99-06-(20→24), pp.135-140.